Environmental Engineering and Management Journal

May 2020, Vol.19, No. 5, 819-828
http://www.eemj.icpm.tuiasi.ro/; http://www.eemj.eu

"Gheorghe Asachi" Technical University of Iasi, Romania

RECYCLING OF LIGHT-EMITTING DIODE WASTE QUARTZ SAND ACTING AS A POZZOLANIC MATERIAL FOR PORTLAND CEMENT

Kae-Long Lin[1*], Kang-Wei Lo[2,3], Wei-Ting Lin[4], Ta-Wui Cheng[3], Wei-Hao Lee[3]

[1]Department of Environmental Engineering, National Ilan University, Ilan City, 260, Taiwan, R.O.C.
[2]Graduate Institute of Engineering Technology, National Taipei University of Technology, Taipei City, 106, Taiwan, R.O. C.
[3]Institute of Mineral Resources Engineering, National Taipei University of Technology, Taipei City, 106, Taiwan, R.O. C.
[4]Department of Civil Engineering, National Ilan University, Ilan City, 260, Taiwan, R.O.C.

Abstract

LED waste quartz sand (LEDWS), which is a prominent by product of the LED manufacturing process, may contaminate the environment because it comprises specific heavy metals (e.g., As and Cu), which are hazardous ingredients to the environment when disposed of improperly. Therefore, this study investigated the use of light-emitting diode (LED) waste quartz sand to partially replace Portland Type I cement (OPC) to evaluate the feasibility of reusing it as a pozzolanic material. The SiO_2, Na_2O, and CaO contents in the LED waste quartz sand were 70.37, 16.52, and 9.19%, respectively. The results showed that the LED waste quartz sand met the Taiwan EPA regulatory thresholds. Microstructure analysis techniques, such as mercury intrusion porosimetry (MIP), X-ray diffraction (XRD) and scanning electron microscopy (SEM), were used to measure the LED waste quartz sand-blended cement paste (LEDBCP) samples. Compressive strength analysis of the pastes containing 10 wt.% LED waste quartz sand showed that the LED waste quartz sand not only acts as a pozzolanic material to increase the density of the microstructure but also improves the compressive strength of the pastes. LEDBCP with LED waste quartz sand exhibited higher intensity diffraction peaks corresponding to calcium silicate hydrate and lower intensity diffraction peaks corresponding to portlandite (CH) compared with ordinary Portland cement samples at an early age. The gel porosity and pore sizes of the LEDBCP increased with increases in the proportion of LED waste quartz sand. LEDBCP with 10-20 wt.% LED waste quartz sand provides a paste with good pozzolanic characteristics.

Keywords: light-emitting diode, microstructure, pozzolanic material, waste quartz sand

Received: July, 2019; Revised final: November, 2019; Accepted: December, 2019; Published in final edited form: May, 2020

1. Introduction

Light-emitting diodes (LEDs) have replaced traditional light sources (e.g., incandescent bulbs and compact fluorescent lamps) in several fields because of their beneficial features, such as energy efficiency, long lifespan, and environmental friendliness (Fang et al., 2018; Zhao et al., 2016). To reduce the environmental burden and save energy, numerous countries-including the USA, Australia, BRIC countries, South Africa, the European Union, and Japan-have implemented legislation to phase out incandescent lamps and use LED lamps (UNEP, 2012). With the expansion of the LED market, large quantities of LED waste are being generated because of the limited lifespans of and rapid updates to electronic products (Wu et al., 2018).

Metals present in LEDs, particularly heavy metals (e.g., As and Cu), may lead to environmental pollution. Thus, LED waste is a crucial worldwide environmental concern. Treatment methods such as landfilling and incineration are not very effective because the stable structure and properties of the materials in the end-of-life LEDs cannot be altered. Green design and manufacturing are the best approaches in waste management (Altun, 2018; El-

*Author to whom all correspondence should be addressed: e-mail: kllin@niu.edu.tw; Phone: +886 9317579; Fax: +886 39364277

Diadamony et al., 2018). In addition, the primary components of LED waste quartz sand are SiO_2 and Al_2O_3. Therefore, LEDWS can be used to replace or partially replace cement to reduce energy consumption and CO_2 emissions. Supplementary cementitious materials have high alumina or silica content, and the water used in Portland cement can be classified as a pozzolanic material.

Any LED lamp consists of several basic materials. When an LED loses its useful properties, the composition of the LED determines the procedure for utilization or recycling: the glass details of a socle are used in branch segments of construction materials or in the production of products from glass; aluminum parts of the casing or cooling radiator are melted and reused in aluminum production; secondary use of the polycarbonate or plastic parts of the housing of the lighting device, base or light diffusers is also assumed.

This article presents studies on the use of the glass waste as a pozzolan additive to cement. However, an alkaline medium is formed through the dissolution of calcium hydroxide in water, and the silicate or aluminosilicate networks break down to form calcium silicate or calcium aluminate hydrates (CSH or CAH) (Papatzani et al., 2018). Mashaly et al. (2018) reported that mortar and concrete mixes containing 20% granite sludge exhibit enhanced resistance to abrasion, sulfate attack, and freeze as well as thaw (Mashaly et al., 2018). Kubiliute et al. (2018) indicated that after 28 and 90 days of hydration, the compressive strength of cement samples with 5, 10 and 15 wt. % mineral wool cupola dust additives were higher than that of ordinary Portland cement (OPC) (Kubiliute et al., 2018). These dust additives lead to the formation of a stable structure, accelerate the hydration of calcium silicate, and promote the formation of gismondine (Kubiliute et al., 2018). Li et al. (2019) reported that the compressive strength of the paste with GGBS increased more quickly after 7 days and was comparable to that of the control paste on the 56th day, at approximately 85.0 MPa. PFA paste possessed only approximately 80% of the strength of the GGBS paste due to the lower pozzolanic reactivity (Li et al., 2019). Demir et al. (2018) demonstrated that the compressive strength of cement mortars that contained 5% blast furnace slag and bottom ash was 2% higher than that of unmodified cement mortars at 360 days (Demir et al., 2018).

In this study, LED waste quartz sand was used as a pozzolan. Because it is mainly composed of SiO_2, a pozzolanic reaction is activated using the alkaline cement. In this reaction, the addition of pozzolan results in the release of KOH, $Ca(OH)_2$, and NaOH, thus producing low-density calcium silicate hydrate (CSH) gels (Schwarz and Neithalath 2008). By slowly filling the pores and thereby improving the internal microstructure of the cement paste, these gels help improve the mechanical properties, chemical resistance, and acid resistance of the cement paste. This results in the reduction of the amount of the cement used, thus reducing the emissions of carbon dioxide and the unit cost of cement production. In this study, the effects of the addition of LED waste quartz sand as a pozzolanic material on the mineral composition and hydration of cement were examined.

This paper assesses the pozzolanic progress in light-emitting diode waste quartz sand-blended cement pastes (LEDBCP) with curing time in terms of the setting time, compressive strength and microstructural characteristics. Chemical composition, crystallinity, morphology, and reactivity of the LEDBCP samples are analyzed by powder X-ray diffraction (XRD), scanning electron microscopy (SEM) and mercury intrusion porosimetry (MIP) methods.

2. Material and methods

2.1. Materials

In this study, cleaning the sapphire substrate of the LEDs using quartz sand through dry etching could increase the internal quantum efficiency and light extraction efficiency of the LED. The polished LED stage is sandblasted using quartz sand, and the polished waste is called LED waste quartz sand. The LED waste quartz sand used in this study was obtained from Optoelectronics Corporation in northern Taiwan. The pH value and specific gravity were set according to NIEA R208.04C pH and ASTM C188, respectively. The LED waste quartz sand had pH, specific gravity, and Blaine fineness values of 9.43, 1.70, and 349.7 m^2/kg, respectively.

The chemical composition of the LED waste quartz sand was determined through X-ray fluorescence measurements (Table 1). The LED waste quartz sand was composed of SiO_2 (70.37%), Na_2O (16.52%), and CaO (9.19%) and could be used as a source material for the pozzolanic reaction. The strength activity index (SAI) of the LED waste quartz sand was used to evaluate the pozzolanicity and was prepared according to ASTM C311-98a. The LED waste quartz sand was observed to have a higher SAI value (102%) as well as pozzolanic effects. The toxicity characteristic leaching procedure (TCLP) test on the LED waste quartz sand was performed according to the NIEA-R201.14C. As shown in Table 2, the leaching concentrations of the LED waste quartz sand satisfied the regulatory thresholds. In this study, numerous samples of waste quartz sand were passed through a 200-mesh sieve to control particle size.

Table 1. Chemical composition of LED waste quartz sand

Composition	***LED Waste Quartz Sand***
SiO_2 (%)	70.37
Al_2O_3 (%)	0.26
Fe_2O_3 (%)	0.06
CaO (%)	9.19
MgO (%)	3.19
SO_3 (%)	0.25
Na_2O (%)	16.52
K_2O (%)	0.12

Table 2. Total Metals and TCLP leaching concentrations of LED waste quartz sand

LED Waste Quartz Sand	***Pb***	***Cr***	***Cu***	***Zn***	***Cd***	***Ni***
Total Metal (mg/kg)	N.D.	N.D.	11.67	48.33	N.D.	38.33
TCLP (mg/L)	N.D.	N.D.	N.D.	0.28	N.D.	N.D.
Regulatory Limits (mg/L)	5.00	5.00	15.00	-	1.00	-

ND : Pb < 0.015 mg/L ; Cr < 0.009 mg/L ; Cd < 0.021 mg/L ; Zn < 0.074 mg/L ; Cu < 0.089 mg/L ; Ni < 0.112 mg/L

2.2. Methods

The LED waste quartz sand used in this study was sieved through a 200-mesh sieve, and its fineness was measured using a Blaine fineness apparatus. All pastes were prepared with a water-to-binder ratio of 0.4. Test cubes (1 × 1 × 1 inch) were prepared according to ASTM C109, and the LED waste quartz sand was replaced at 0.0, 10, 20, 30, and 40 wt.% (Table 1). The samples were demoulded after 24 h; subsequently, curing was performed in a saturated calcium carbonate solution at 30 ± 2 °C for various durations.

According to ASTM C39-72, compressive strength tests were performed on three samples at curing ages of 7, 14, 28, 56, and 90 days. Subsequently, the broken samples were prepared for other analyses by immersing the specimens in methanol to terminate hydration and then dried at 105 °C for 24 h. Cement paste samples were extracted to determine setting times using a Vicat apparatus according to ASTM C191 (Abolpour et al., 2015). Finally, the samples were analysed at the specified curing ages through MIP, XRD, and SEM. Three specimens were used for the compressive strength tests, while the microstructure was evaluated in the fourth. The average strength of the three specimens is presented. The coefficient of variation of these results was less than 10%.

3. Results and discussion

3.1. Setting times of the LEDBCP with LED waste quartz sand

The variations of setting times of the LEDBCP with LED waste quartz sand are graphically represented in Fig. 1. The setting times of LEDBCP increased with an increase in the proportion of LED waste quartz sand. Relative to that for OPC, the final setting times for the LEDBCP with 10, 20, 30, and 40 wt.% LED waste quartz sand increased by 30, 45, 65, and 105 min, respectively. These results indicate that LEDBCP with 40 wt.% LED waste quartz sand has significantly increased setting time compared with LEDBCP with 10-30 wt.% LED waste quartz sand. This performance was attributed to the lower cement content in the mixture, which resulted in less formation of the primary calcium silicate hydrate structure in the matrix (Ismail et al., 2020).

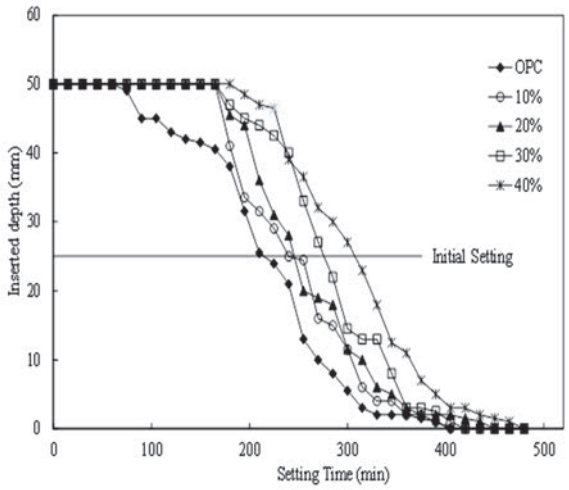

Fig. 1. Setting times of the LEDBCP with LED waste quartz sand

3.2. Compressive strength of LEDBCP with LED waste quartz sand

Fig. 2 illustrates the compressive strength of LEDBCP with LED waste quartz sand. LEDBCP with 10 wt.% LED waste quartz sand performed with a compressive strength similar to that of OPC at later ages. The pozzolanic reactivity of the LED waste quartz sand (i.e., relative strengths of 98.6%-87.8% at 90 days compared with the OPC pastes) exhibited by the pastes containing 10-20 wt.% LED waste quartz sand was significantly higher than that of OPC. Zhou et al. (2019) reported that the compressive strength of OPC-ISSA pastes gradually increased with increasing curing age and total binder content.

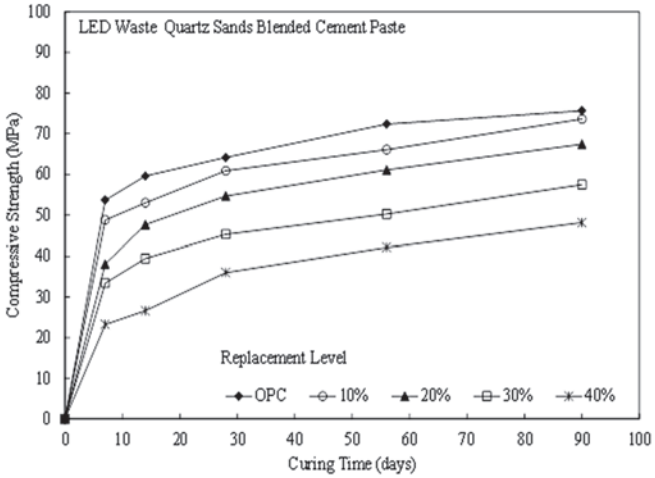

Fig. 2. Compressive strength of LEDBCP with LED waste quartz sand

This was mainly attributed to OPC hydration and the pozzolanic reaction between the CH formed from OPC hydration and ISSA (Zhou et al., 2019). With an increasing number of treatment days, the intensity of the pastes that incorporated 10% LEDWS approached that of the OPC, in agreement with Zhou et al. (2019). LED waste quartz sand with $Ca(OH)_2$

exerts a nucleation effect as well as pozzolanic effects, leading to the accumulation and precipitation of the hydrated products in the open pores and to the formation of the denser microstructure (Abd-El-Aleem et al., 2014). The low rate of strength development for LEDBCP with 10-20 wt% LED waste quartz sand is related to the state of the LED waste quartz sand, as the samples were supplied in a densified form at later ages (Sanchez de Rojas et al., 1999). The LEDBCP with 30%-40% LED waste quartz sand was apparently observed to have lower compressive strengths relative to OPC at curing ages of 7-90 days.

This observation reveals that the hydration of the LED waste quartz sand particles for the LEDBCP with 40% LED waste quartz sand, consumption of the formed hydration products, and production of these hydrates maintains the porosity of the samples at various curing ages (Zeng et al., 2012). This observation is similar to that of Poon et al. (2001) for high-performance cement pastes (Poon et al., 2001).

3.3. X-ray diffractograms of LEDBCP with LED waste quartz sand

Fig. 3 displays X-ray diffractograms of OPC hydrated for 7-90 days. The main hydration products after various curing times were portlandite, tobermorite, calcium silicate hydrate (C-S-H), ettringite, and anhydrous C_3S and β-C_2S. By increasing the curing time, the diffraction peaks corresponding to portlandite had a higher intensity, and the main diffraction peaks were located at 17.97°, 34.02°, and 46.96° (Table 3).

Fig. 4 depicts the X-ray diffractograms of LEDBCP with LED waste quartz sand hydrated for 7-90 days. The intensity of the portlandite peak and anhydrous silicate phases (β-C_2S and C_3S) decreased with increasing LED waste quartz sand content at later ages, whereas the diffraction peaks corresponding to the tobermorite-like phase increased with increasing LED waste quartz sand content. It is possible that the pozzolanic reaction of the LED waste quartz sand with portlandite forms a tobermorite-like phase. In LEDBCP with LED waste quartz sand, a hydration reaction occurs between the portlandite, which is the hydration product of LEDBCP, and the LED waste quartz sand.

With time, the amount of free calcium hydroxide decreased gradually. The hydration reaction is similar to an acid–base reaction of portlandite and alkalis with SiO_2 in LEDBCP (Askarinejad et al., 2012). At later ages, during the pozzolanic reaction, the formation of stable crystals of C-S-H and C-A-H increased, increasing the compressive strength of the LEDBCP with LED waste quartz sand.

Fig. 4 presents the XRD diffraction patterns of the LEDBCP with LED waste quartz sand hydrated for up to 90 days. Compared with the tobermorite-like gel phase, the peaks of portlandite decreased with increasing curing time. This decrease is because of the progress of the hydration and the pozzolanic reaction of the LEDBCP with LED waste quartz sand with portlandite, leading to the increased formation of C-S-H. The peaks related to the formation of the hydrated products shift and appear at earlier curing ages, indicating the positive effect of the LEDBCP with LED waste quartz sand on the formation of $Ca(OH)_2$, C-S-H and C-A-H at later curing ages (Abd-El-Aleem et al., 2014). This is because the pozzolanic reaction started to take effect by producing a secondary calcium silicate hydrate matrix and producing pastes (Ismail et al., 2020).

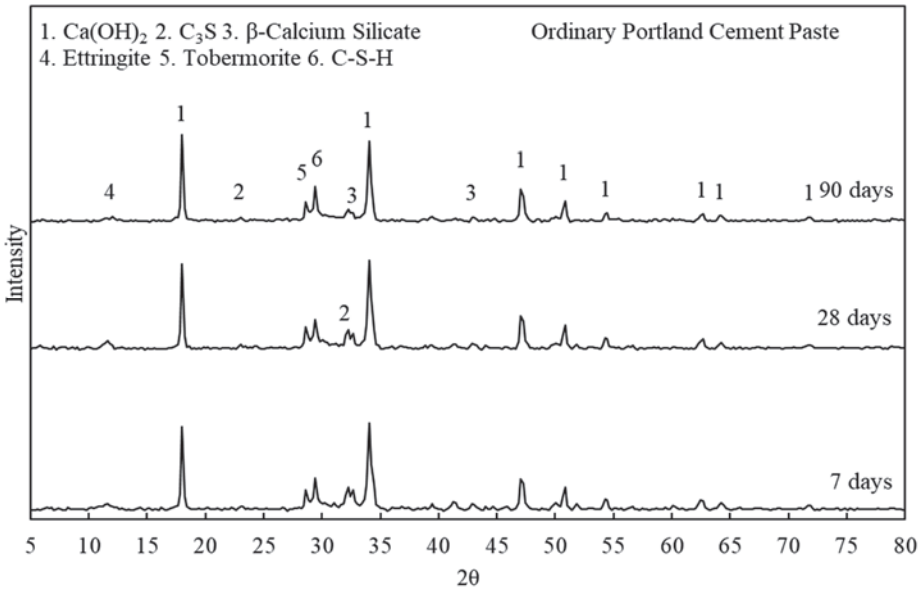

Fig. 3. X-ray diffractograms of OPC samples

Table 3. X-ray diffractograms intensity of LEDBCP with 0%-40% LED waste quartz sand

Replacement Level (%)	***Curing days***	***Intensity***		
		17.97°	***34.02°***	***46.96°***
0	7	4341	4509	1914
0	28	11950	12130	9475
0	90	17973	17668	15461
10	7	5103	4610	2060
10	28	11898	11935	9412
10	90	17419	17805	5281
20	7	4724	4733	2001
20	28	11826	11781	9453
20	90	16702	17056	14890
30	7	4685	4531	1927
30	28	11619	11585	9351
30	90	16287	16719	14976
40	7	4259	4341	1803
40	28	11874	11349	9225
40	90	15775	16078	14781

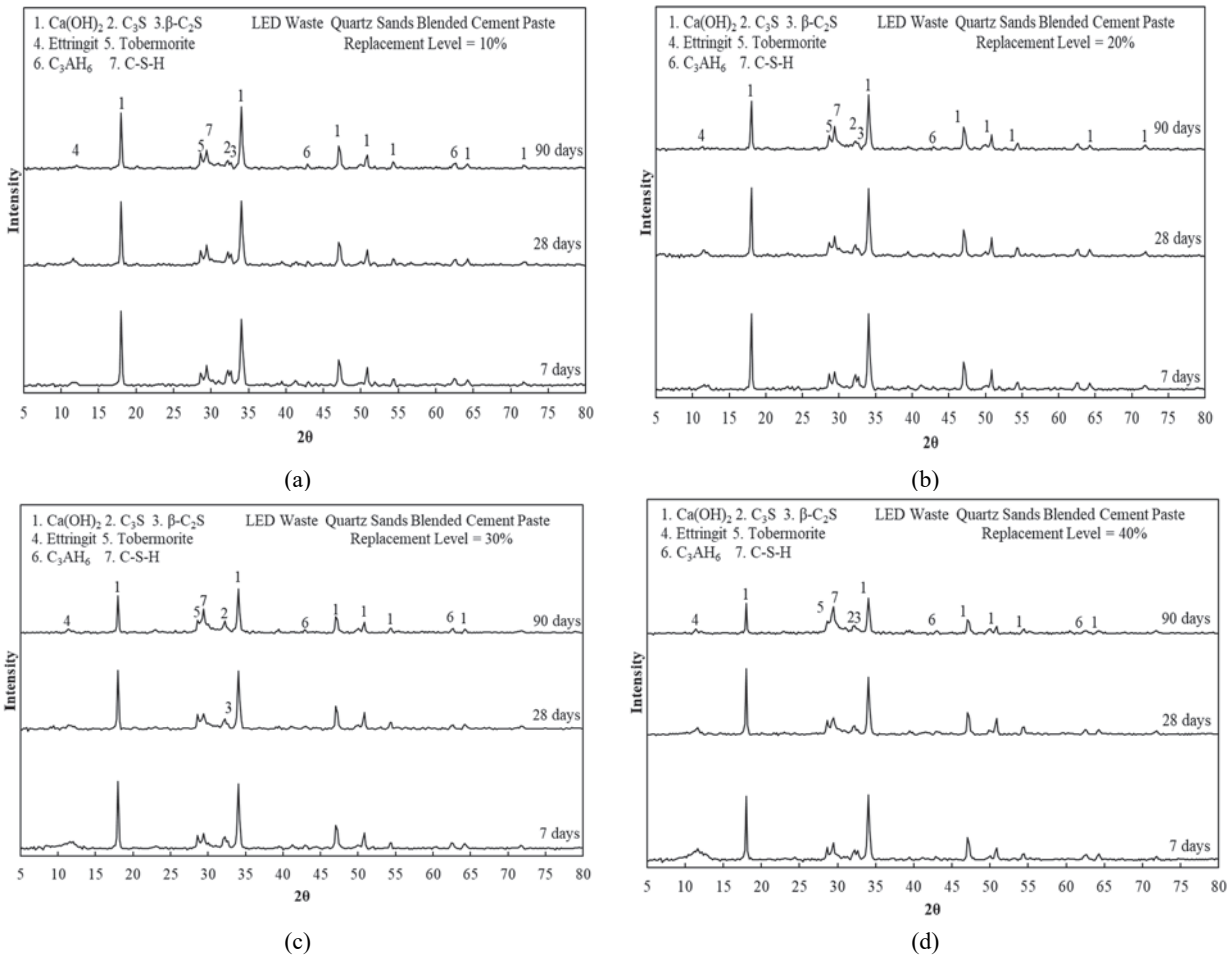

Fig. 4. X-ray diffractograms of LEDBCP with LED waste quartz sand: (a) Replacement Level=10%; (b) Replacement Level=20%; (c) Replacement Level=30%; (d) Replacement Level=40%

3.4. Mercury porosimetry of LEDBCP with LED waste quartz sand

Fig. 5 shows the pore size distribution of the OPC samples and the LEDBCP with LED waste quartz sand at 7, 28 and 90 days. The pore size distribution of the OPC samples was approximately 0.1–0.01 μm at 7 days of curing. As expected, with an increase in the curing time, the total porosities of the OPC pastes decreased. The pore size distribution shifted lower, with the distribution changing from 0.1-0.01 μm to 5-12 nm after 90 days of curing. The initial peak may correspond to the intrusion of mercury through a connected capillary network, whereas the rounded peak may correspond to the hydrated LEDBCP products (Cook and Hover., 1999; Lu et al.,

2018).

Fig. 5 illustrates the pore size distribution of the LEDBCP with LED waste quartz sand at 7, 28 and 90 days of curing. The pore size distribution of the LEDBCP with LED waste quartz sand started from approximately 0.1 μm at the 7-day curing age. As expected, an increase in the curing time reduced the total porosities of the OPC pastes. The pore size distribution narrowed at a 90-day curing age, with pores of diameter 0.1 μm transforming to pores of 0.01 μm. The presence of a sharp intrusion peak indicated the intrusion of mercury throughout the LEDBCP samples through a pore network connected to the LEDBCP sample surfaces (Lu et al., 2018; Mashaly et al., 2018; Xu et al., 2018).

Fig. 6 and Table 4 depict the pore volume of LEDBCP with LED waste quartz sand. For LEDBCP with 10-40 wt% LED waste quartz sand, the total porosity increased with an increase in the proportion of LED waste quartz sand. As expected, the total porosity values of the LEDBCP with 10-40 wt% LED waste quartz sand after 28 days of curing were approximately 0.148-0.286 mL/g higher than that for OPC pastes (0.0835 mL/g). For the LEDBCP with 20 and 40 wt% LED waste quartz sand, the increase in total porosity relative to that of the OPC pastes was 0.1 and 0.2 mL/g, respectively. LEDBCP with 40% LED waste quartz sand at 28 days of curing demonstrated higher total porosity than did the OPC pastes, indicating lower pozzolanic activity at an early age. However, the pore structure was refined for the LEDBCP with 10-40 wt% LED waste quartz sand at a later age. The gel porosity values were 0.0248-0.0827 mL/g higher than that of the OPC paste (0.0066 mL/g) at 90 days of curing. For the LEDBCP with 20 and 40 wt% LED waste quartz sand, the increase in gel porosity reached 0.029 and 0.076 mL/g, indicating that the LEDBCP with 10-20 wt% LED waste quartz sand used in this study was more effective than OPC in refining the pore structure of the LEDBCP samples. The gel porosity of the LEDBCP increased with an increase in the proportion of LED waste quartz sand.

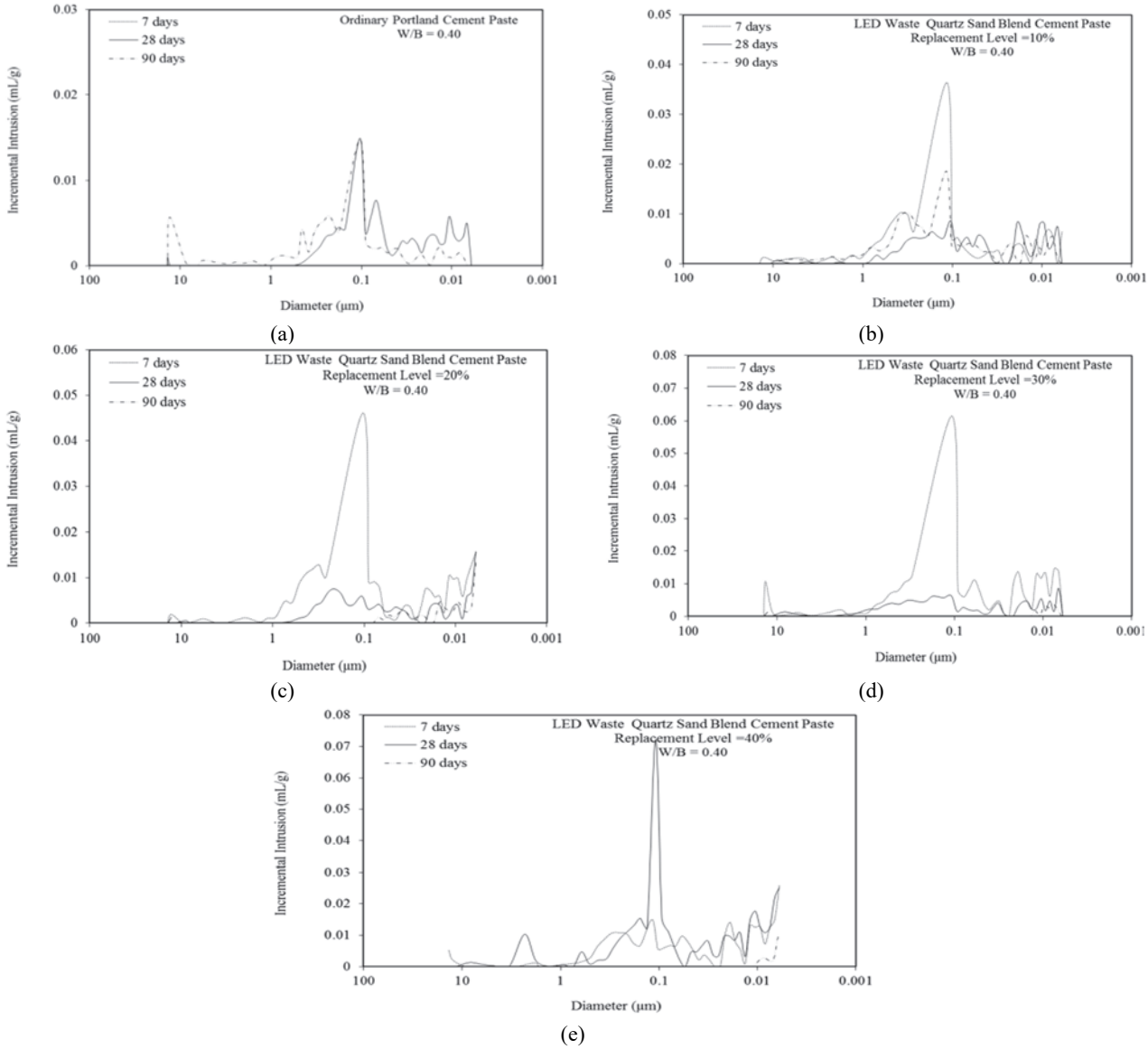

Fig. 5. Pore size distribution of LEDBCP with 10%-40% LED waste quartz sand: (a) Replacement Level=0%; (b) Replacement Level=10%; (c) Replacement Level=20%; (d) Replacement Level= 30%; (e) Replacement Level=40%

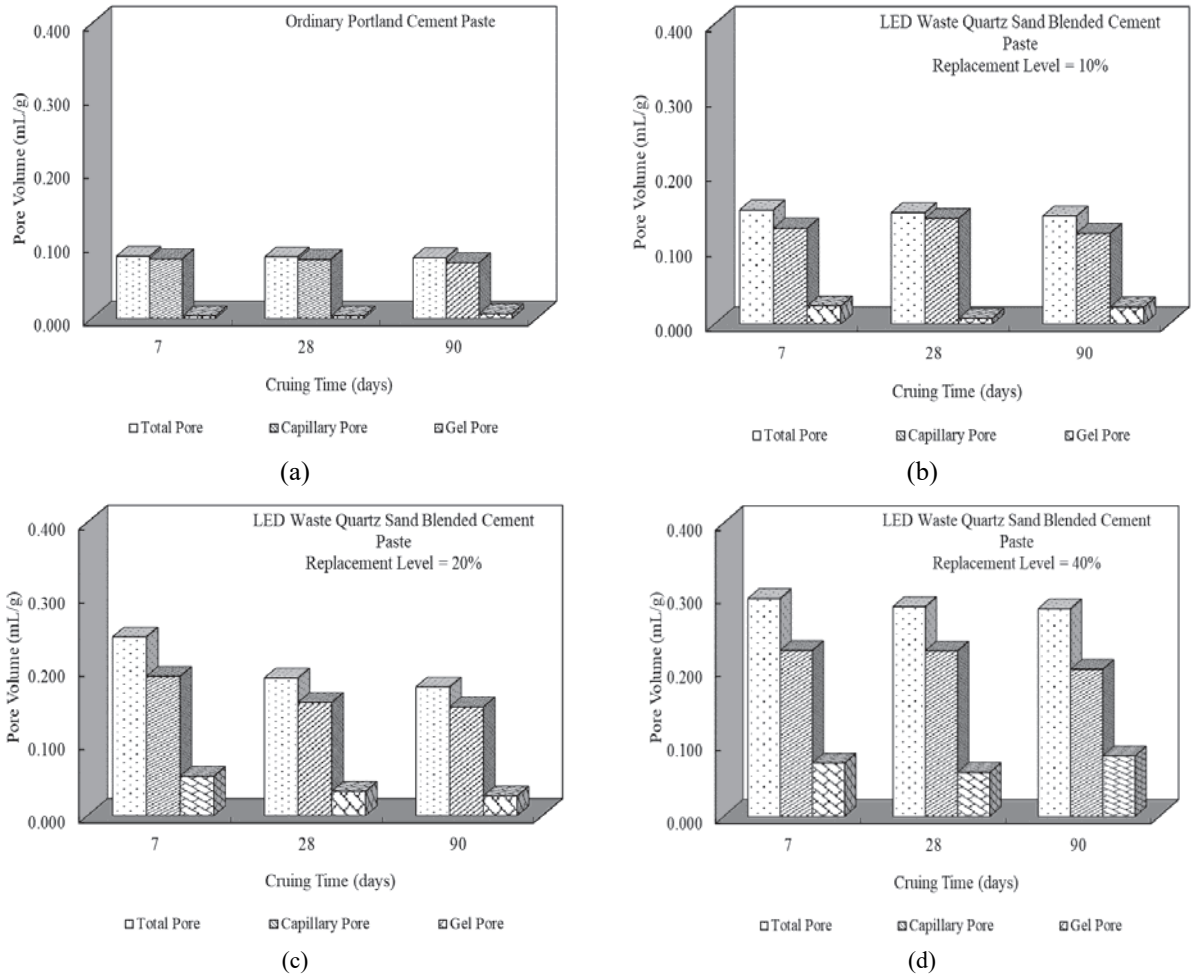

Fig. 6. Pore volume of LEDBCP with LED waste quartz sand: (a) Replacement Level=0%; (b) Replacement Level=10%; (c) Replacement Level=20%; (d) Replacement Level=40%

Table 4. Pore volume of LEDBCP with LED waste quartz sand

Replacement Level (%)	***Curing days***	***Total Pore (mL/g)***	***Capillary Pore (mL/g)***	***Gel Pore (mL/g)***
0	7	0.084	0.081	0.003
0	28	0.084	0.080	0.003
0	90	0.082	0.076	0.007
10	7	0.152	0.128	0.024
10	28	0.149	0.141	0.008
10	90	0.144	0.121	0.023
20	7	0.244	0.190	0.054
20	28	0.188	0.154	0.033
20	90	0.175	0.148	0.027
40	7	0.297	0.226	0.073
40	28	0.286	0.226	0.060
40	90	0.283	0.201	0.083

3.5. SEM micrographs of LEDBCP with LED waste quartz sand

Figs. 7-8 depict SEM micrographs of LEDBCP with 10-40 wt% LED waste quartz sand hydrated for 28 days and 90 days, respectively.

A denser structure was observed for the LEDBCP with 10-20 wt% LED waste quartz sand after 28 days of curing. The structure is mainly composed of gel-like C-S-H. It is possible that LED waste quartz sand reacts with portlandite liberated from the process of C_3S and β-C_2S hydration to form C-S-H, in agreement with the X-ray diffractogram intensity analysis.

The formation of C-S-H in large quantities creates bridges of LEDBCP particles, producing a

rigid system, which explains how the compressive strength of these pastes is similar to that of OPCs. The large quantity of C-S-H indicates that the LEDBCP with 10‑20 wt% LED waste quartz sand has a higher hydration and strength due to its relatively low porosity, in agreement with pore volume analysis. The LED waste quartz sand particles occupy the gel pores, and the C-S-H gel growth inhibits the strength of the LEDBCP (Ghabezloo et al., 2009; Wu and Lian, 1999; Xijun and Mingwen, 1997). With an increase in the LED waste quartz sand content, the hydration products decrease considerably.

However, with increasing curing time, the structure becomes denser. LEDBCP with 10-20 wt% LED waste quartz sand forms a more uniform and denser microstructure than does that with 40% LED waste quartz sand at 28 days of curing. LEDBCP with 10-20 wt% LED waste quartz is pozzolanic and exhibits high-strength characteristics

4. Conclusions

The compressive strength of the LEDBCP with 10-20 wt.% LED waste quartz sand indicates that the LED waste quartz sand can act as a pozzolanic material to improve the LEDBCP microstructure. Calcium silicate hydrate increased with increasing curing time because of the progress of hydration and the pozzolanic reaction of the LEDBCP with LED waste quartz sand with $Ca(OH)_2$, leading to the increased formation of C-S-H.

For the LEDBCP with 10-40 wt.% LED waste quartz sand, the gel porosity values were 0.0248-0.0827 mL/g higher than that of the OPC pastes (0.0066 mL/g) at 90 days of curing, indicating that the LEDBCP with 10-20 wt.% LED waste quartz sand used in this study was more effective than OPC in refining the pore structure of the LEDBCP samples.

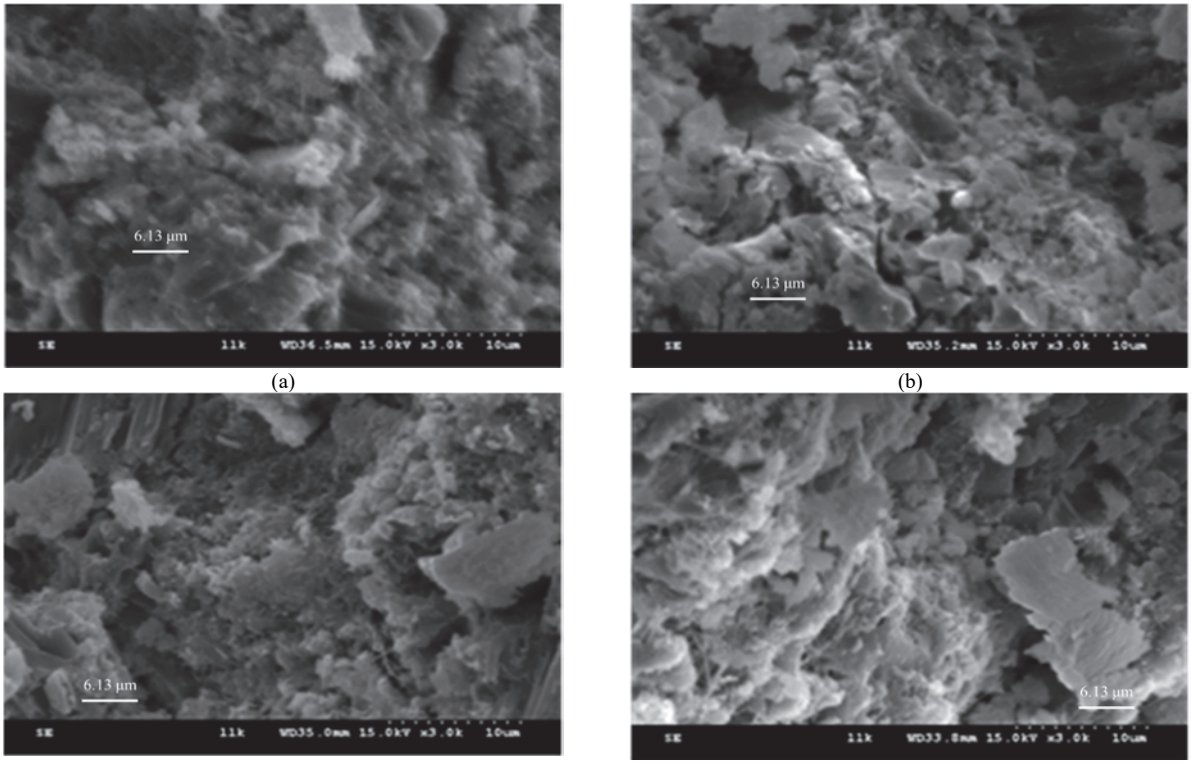

(a) (b) (c) (d)

Fig. 7. SEM micrographs of LEDBCP with LED waste quartz sand (28 days): (a) Replacement Level=0%; (b) Replacement Level=10%; (c) Replacement Level=20%; (d) Replacement Level=40%

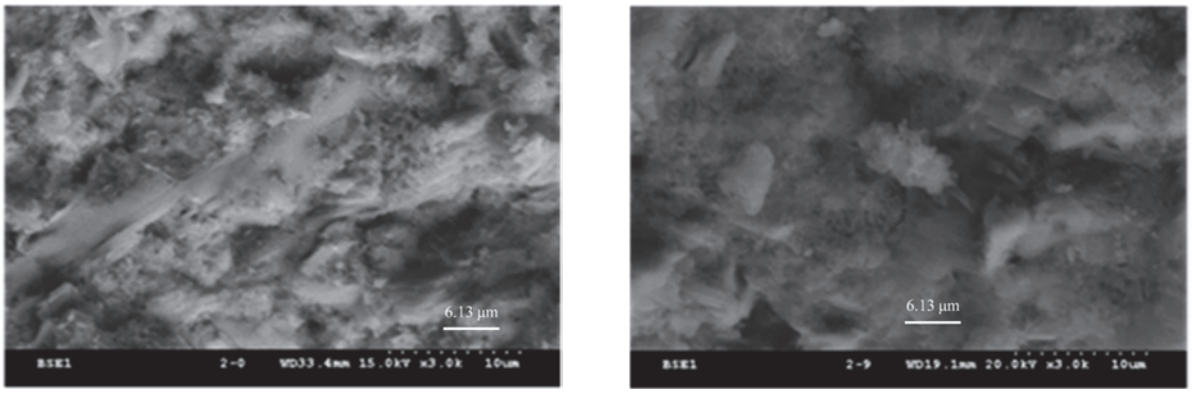

(a) (b)

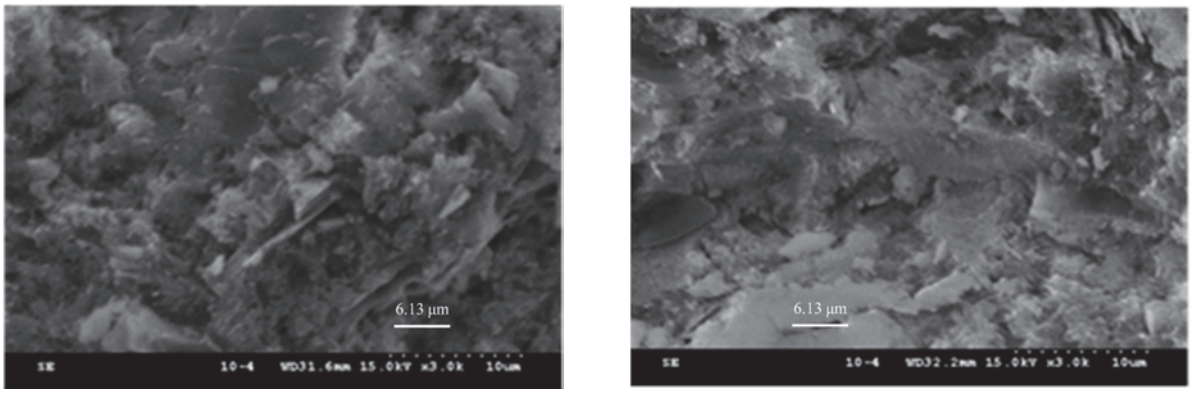

(c) (d)

Fig. 8. SEM micrographs of LEDBCP with LED waste quartz sand (90 days): (a) Replacement Level=0%; (b) Replacement Level=10%; (c) Replacement Level=20%; (d) Replacement Level=40%

LEDBCP with 10-20 wt% LED waste quartz sand forms a more uniform and denser microstructure than does that with 40 wt.% LED waste quartz sand at 28 days of curing and is pozzolanic and exhibits high-strength characteristics.

References

Abd-El-Aleem S., Heikal M., Morsi W.M., (2014), Hydration characteristic, thermal expansion and microstructure of cement containing nano-silica, *Construction and Building Materials*, **59**, 151-160.

Abolpour B., Afsahi M.M., Hosseini S.G., (2015), Statistical analysis of the effective factors on the 28 days compressive strength and setting time of the concrete, *Journal of Advanced Research*, **6**, 699-709.

Altun O., (2018), Energy and cement quality optimization of a cement grinding circuit, *Advanced Powder Technology*, **29**, 1713-1723.

Askarinejad A., Pourkhorshidi A.R., Parhizkar T., (2012), Evaluation the pozzolanic reactivity of sonochemically fabricated nano natural pozzolan, *Ultrasonics Sonochemistry*, **19**, 119-124.

Cook R.A., Hover K.C., (1999), Mercury porosimetry of hardened cement pastes, *Cement and Concrete Research*, **29**, 933-943.

Demir I., Güzelkücük S., Sevim Ö., (2018), Effects of sulfate on cement mortar with hybrid pozzolan substitution, *Engineering Science and Technology*, *an International Journal*, **21**, 275-283.

El-Diadamony H., Amer A.A., Sokkary T.M., El-Hoseny S., (2018), Hydration and characteristics of metakaolin pozzolanic cement pastes, *HBRC Journal*, **14**, 150-158.

Fang S., Yan W., Cao H., Song Q., Zhang Y., Sun Z., (2018), Evaluation on end-of-life LEDs by understanding the criticality and recyclability for metals recycling, *Journal of Cleaner Production*, **182**, 624-633.

Ghabezloo S., Sulem J., Saint-Marc J., (2009), The effect of undrained heating on a fluid-saturated hardened cement paste, *Cement and Concrete Research*, **39**, 54-64.

Ismail A.H., Kusbiantoro A., Chin S.C., Muthusamy K., Islam M., Tee K.F., (2020), Pozzolanic reactivity and strength activity index of mortar containing palm oil clinker pretreated with hydrochloric acid, *Journal of Cleaner Production*, **242**, 118565.

Kubiliute R., Kaminskas R., Kazlauskaite A., (2018), Mineral wool production waste as an additive for Portland cement, *Cement and Concrete Composites*, **88**, 130-138.

Li B., Ling T.C., Yu J.G., Wu J.Q., Chen W.W., (2019), Cement pastes modified with recycled glass and supplementary cementitious materials: Properties at the ambient and high temperatures, *Journal of Cleaner Production*, **241**, 118155.

Lu B., Shi C., Zhang J., Wang J., (2018), Effects of carbonated hardened cement paste powder on hydration and microstructure of Portland cement, *Construction and Building Materials*, **186**, 699-708.

Mashaly A.O., Shalaby B.N., Rashwan M.A., (2018), Performance of mortar and concrete incorporating granite sludge as cement replacement, *Construction and Building Materials*, **169**, 800-818.

Papatzani S., Badogiannis E.G., Paine K.A., (2018), The pozzolanic properties of inorganic and organomodified nano-montmorillonite dispersions, *Construction and Building Materials*, **167**, 299-316.

Poon C.S., Lama L., Kou S.C., Wong Y.L., Wong R., (2001), Rate of pozzolanic reaction of metakaolin in high-performance cement pastes, *Cement and Concrete Research*, **31**, 1301-1306.

Sanchez de Rojas M.I., Rivera J., Frias M., (1999), Influence of the microsilica state on pozzolanic reaction rate, *Cement and Concrete Research*, **29**, 945-949.

Schwarz N., Neithalath N., (2008), Influence of a fine glass powder on cement hydration: Comparison to fly ash and modeling the degree of hydration, *Cement and Concrete Research*, **38**, 429-436.

UNEP, (2012), UNEP highlights benefits of switching to efficient lighting, The United Nation's en.lighten initiative is encouraging developing and emerging nations to phase out inefficient lighting, with an emphasis on the financial and social benefits, 2. 07. 2012, On line at: https://www.ledsmagazine.com/home/article/1670117 7/unep-highlights-benefits-of switching-to-efficient-lighting.

Wu M., Zhang Y.S., Ji Y.S., Liu G.J., Liu C., She W., Sun W., (2018), Reducing environmental impacts and carbon emissions: Study of effects of superfine cement particles on blended cement containing high volume mineral admixtures, *Journal of Cleaner Production*, **196**, 358-369.

Wu Z.W., Lian H.Z., (1999), *High Performance Concrete*, China Railway Publishing House, Beijing.

Xijun W., Mingwen Z., (1997), Properties and interfacial microstructures for nanostructured materials, *Journal of Atomic and Molecular Physics*, **2**, 148-152.

Xu F., Wei H., Qian W.X., Cai Y.B., (2018), Composite alkaline activator on cemented soil: Multiple tests and

mechanism analyses, *Construction and Building Materials*, **188**, 433-443.

Zeng Q., Li K., Fen-chong T., Dangla P., (2012), Pore structure characterization of cement pastes blended with high-volume fly-ash, *Cement and Concrete Research*, **42**, 194-204.

Zhao L.X., Zhu S.C., Wu C.H., Yang C., Yu Z.G., Yang H., Liu L., (2016), GaN-based LEDs for light communication, *Science China Physics*, *Mechanics and Astronomy*, **59**, 107301.

Zhou Y.F., Li J.S., Lu J.X., Cheeseman C., Poon, C.S., (2019), Recycling incinerated sewage sludge ash (ISSA) as a cementitious binder by lime activation, *Journal of Cleaner Production*, **244**, 1-10.